

Editorial Manager(tm) for AJSE-Mathematics
Manuscript Draft

Manuscript Number: AJSE-MATH-D-10-00104R1

Title: Effects of thermal diffusion and diffusion thermo on chemically reacting MHD boundary layer flow of heat and mass transfer past a moving vertical plate with suction/injection

Article Type: Research Paper

Section/Category: 76 : Fluid mechanics

Keywords: Free convection; Magneto-hydrodynamics (MHD); Chemical reaction; Heat and mass transfer; Dufour and Soret effects; Moving porous plate.

Corresponding Author: Philip Oladapo Oladapo Olanrewaju, PhD

Corresponding Author's Institution:

First Author: Philip Oladapo Oladapo Olanrewaju, PhD

Order of Authors: Philip Oladapo Oladapo Olanrewaju, PhD; Oluwole Daniel Makinde, PhD

Abstract: Analysis is carried out to study free convective heat and mass transfer of an incompressible, electrically conducting fluid past a moving vertical plate in the presence of suction and injection with thermal diffusion (Soret) and diffusion-thermo (Dufour) effects. Similarity solutions are obtained using scaling transformations. Furthermore, using a similarity variable, the governing non-linear partial differential equations have been transformed into a set of coupled non-linear ordinary differential equations, which are solved numerically by applying shooting iteration technique together with sixth order Runge-Kutta integration scheme. A comparison with previously work is performed and the results are found to be in good agreement. Numerical results of the local skin friction coefficient, the local Nusselt number and the local Sherwood number as well as the velocity, the temperature and the concentration profiles are presented for different physical parameters. The result indicates: (i) for fluids with medium molecular weight (H₂, air), Dufour and Soret effects should not be neglected; and (ii) the suction and injection parameter has significant impact in controlling the rate of heat transfer in the boundary layer. Finally, numerical values of physical quantities, such as the local skin-friction coefficient, the local Nusselt number and the local Sherwood number are presented in tabular form.

1
2
3
4 **Effects of thermal diffusion and diffusion thermo on chemically reacting MHD boundary**
5 **layer flow of heat and mass transfer past a moving vertical plate with suction/injection**
6

7
8 ***Olanrewaju, Philip Oladapo and **Makinde Oluwole Daniel**
9

10 *Department of Mathematics, Covenant University, Ota, Ogun State. Nigeria
11

12 **Faculty of Engineering, Cape Peninsula University of Technology, Cape Town. South Africa
13

14 oladapo_anu@yahoo.ie ; makinded@cput.za.ca
15
16
17
18

19 **Abstract**
20

21 Analysis is carried out to study free convective heat and mass transfer of an incompressible,
22 electrically conducting fluid past a moving vertical plate in the presence of suction and injection
23 with thermal diffusion (Soret) and diffusion-thermo (Dufour) effects. Similarity solutions are
24 obtained using scaling transformations. Furthermore, using a similarity variable, the governing
25 non-linear partial differential equations have been transformed into a set of coupled non-linear
26 ordinary differential equations, which are solved numerically by applying shooting iteration
27 technique together with sixth order Runge-Kutta integration scheme. A comparison with
28 previous work is performed and the results are found to be in good agreement. Numerical results
29 for the local skin friction coefficient, the local Nusselt number and the local Sherwood number as
30 well as the velocity, the temperature and the concentration profiles are presented for different
31 physical parameters. The result indicates: (i) for fluids with medium molecular weight (H_2 , air),
32 Dufour and Soret effects should not be neglected; and (ii) the suction and injection parameter has
33 significant impact in controlling the rate of heat transfer in the boundary layer. Finally, numerical
34 values of physical quantities, such as the local skin-friction coefficient, the local Nusselt number
35 and the local Sherwood number are presented in tabular form.
36
37
38
39
40
41
42
43
44
45
46
47
48

49 **Keywords:** Free convection; Magneto-hydrodynamics (MHD); Chemical reaction; Heat and
50 mass transfer; Dufour and Soret effects; Moving porous plate.
51
52
53
54

55 (* email of the corresponding author: Oladapo_anu@yahoo.ie)
56
57
58
59
60
61
62
63
64
65

1. Introduction

Transport of heat through a porous medium has been the subject of many studies due to the increasing need for a better understanding of the associated transport processes. This interest stems from the numerous practical applications which can be modeled or can be approximated as transport through porous media such as packed sphere beds, high performance insulation for buildings, chemical catalytic reactors, grain storage, migration of moisture through the air contained in fibrous insulations, heat exchange between soil and atmosphere, sensible heat storage beds and beds of fossil fuels such as oil shale and coal, salt leaching in soils, solar power collectors, electrochemical processes, insulation of nuclear reactors, regenerative heat exchangers and geothermal energy systems and many other areas. Literature concerning convective flow in porous media is abundant. Representative studies in this area may be found in the recent books by Nield and Bejan [1], Ingham and Pop [2], Vafai [3], Pop and Ingham [4], Ingham et al. [5], Bejan et al. [6], Vadasz [7], etc.

The problem of steady hydromagnetic flow and heat transfer over a stretching surface could be very practicable in many applications in the polymer technology and metallurgy. In particular, many metallurgical processes involve the cooling of continuous strips or filaments by drawing them through a quiescent fluid and that in the process of drawing, these strips are sometimes stretched. In the case of annealing and thinning of copper wires, the properties of the final product depend to a great extent on the rate of cooling. By drawing such strips in an electrically conducting fluid subject to a magnetic field, the rate of cooling can be controlled and final products of desired characteristics might be achieved [8]. And also, in several engineering processes, materials manufactured by extrusion processes and heat treated materials traveling between a feed roll and a wind up roll on convey belts possess the characteristics of a moving continuous surface. The steady flow on a moving continuous flat surface was first considered by Sakiadis [9] who developed a numerical solution using a similarity transformation. Chiam [10] reported solutions for steady hydromagnetic flow over a surface stretching with a power law velocity with the distance along the surface.

Makinde [11-14] have presented some works on the subject of magneto-hydrodynamics (MHD) convection in porous medium. The problem of magneto-hydrodynamics natural convection about a vertical impermeable flat plate can be found in Sparrow and Cess [15], Yih [16] studied the

1
2
3
4 free convection effect on MHD coupled heat and mass transfer of a moving permeable vertical
5 surface. Alan and Rahman [17], examined Dufour and Soret effects on mixed convection flow
6 past a vertical porous flat plate with variable suction embedded in a porous medium for a
7 hydrogen-air mixture as the non-chemical reacting fluid pair. Gaikwad et al. [18], investigated
8 the onset of double diffusive convection in a two component couple stress fluid layer with Soret
9 and Dufour effects using both linear and non-linear stability analysis. Emmanuel et al. [19]
10 studied numerically the effect of thermal-diffusion and diffusion-thermo on combined heat and
11 mass transfer of a steady hydromagnetic convective and slip flow due to a rotating disk with
12 viscous dissipation and Ohmic heating. Anwar et al. [20] examined the combined effects of Soret
13 and Dufour diffusion and porous impedance on laminar magneto-hydrodynamic mixed
14 convection heat and mass transfer of an electrically-conducting, Newtonian, Boussinesq fluid
15 from a vertical stretching surface in a Darcian porous medium under uniform transverse
16 magnetic field. Nithyadevi and Yang [21] investigated numerically the effect of double-diffusive
17 natural convection of water in a partially heated enclosure with Soret and Dufour coefficients
18 around the density maximum. Olanrewaju [22] examined Dufour and Soret Effects of a Transient
19 Free Convective Flow with Radiative Heat Transfer Past a Flat Plate Moving through a Binary
20 Mixture. Recently, Ibrahim and Makinde [23] studied the combined effects of wall suction and
21 magnetic field on boundary layer flow with heat and mass transfer over an accelerating vertical
22 plate. The present communication considers the effects of Dufour and Soret on a free convection
23 of a continuously moving porous vertical surface as presented in [23]. It investigates numerically
24 the effects of heat and mass transfer in a hydromagnetic boundary layer flow of a moving
25 vertical porous plate with uniform heat generation, chemical reaction with Dufour and Soret in
26 the presence of suction/injection. By using scaling transformations, the set of governing
27 equations and the boundary conditions are reduced to non-linear ordinary differential equations
28 with appropriate boundary conditions. Furthermore, the similarity equations are solved
29 numerically by using shooting technique with sixth-order Runge-Kutta integration scheme.
30 Numerical results of the local skin friction coefficient and the local Nusselt number as well as the
31 velocity, temperature and concentration profiles are presented for different physical parameters.
32
33
34
35
36
37
38
39
40
41
42
43
44
45
46
47
48
49
50
51
52
53
54
55
56
57
58
59
60
61
62
63
64
65

2. Governing equations

We consider the steady free convective heat and mass transfer flow of a viscous, incompressible and electrically conducting fluid past a moving vertical plate with suction/injection in the presence of thermal diffusion (Soret) and diffusion-thermo (Dufour) effects (see Fig. 1) The non-uniform transverse magnetic field B_o is imposed along the y-axis. The induced magnetic field is neglected as the magnetic Reynolds number of the flow is taken to be very small. It is also assumed that the external electric field is zero and the electric field due to polarization of charges is negligible. The temperature and the concentration of the ambient fluid are T_∞ and C_∞ , and those at the surface are $T_w(x)$ and $C_w(x)$, respectively.

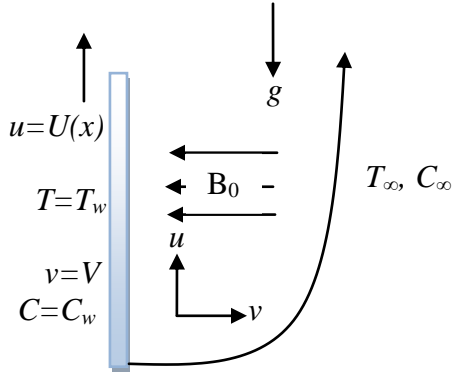


Fig.1: Physical configuration and coordinate system

It is also assumed that the pressure gradient, viscous and electrical dissipation are neglected. The fluid properties are assumed to be constant except the density in the buoyancy terms of the linear momentum equation which is approximated according to the Boussinesq's approximation. Under the above assumptions, the boundary layer form of the governing equation can be written as (see Ref. [24])

$$\frac{\partial u}{\partial x} + \frac{\partial v}{\partial y} = 0 \quad (1)$$

$$u \frac{\partial u}{\partial x} + v \frac{\partial u}{\partial y} = \nu \frac{\partial^2 u}{\partial y^2} + g\beta_T(T - T_\infty) + g\beta_C(C - C_\infty) - \frac{\sigma B_o^2}{\rho} u \quad (2)$$

$$u \frac{\partial T}{\partial x} + v \frac{\partial T}{\partial y} = \alpha \frac{\partial^2 T}{\partial y^2} + \frac{D_m k_T}{c_s c_p} \frac{\partial^2 C}{\partial y^2} \quad (3)$$

$$u \frac{\partial C}{\partial x} + v \frac{\partial C}{\partial y} = D_m \frac{\partial^2 C}{\partial y^2} + \frac{D_m k_T}{T_m} \frac{\partial^2 T}{\partial y^2} \quad (4)$$

The boundary conditions for Eqs. (1)-(4) are expressed as

$$\begin{aligned} v=V, u=Bx, T=T_w=T_\infty+ax, C=C_w=C_\infty+bx \text{ at } y=0, \\ u \rightarrow 0, T \rightarrow T_\infty, C \rightarrow C_\infty \text{ as } y \rightarrow \infty, \end{aligned} \quad (5)$$

where B is a constant, a and b denotes the stratification rate of the gradient of ambient temperature and concentration profiles, (u, v) are the velocity components in x - and y - directions, respectively, T is the temperature, β_T is the volumetric coefficient of thermal expansion, α is the thermal diffusivity, g is the acceleration due to gravity, ν is the kinematic viscosity, D_m is the coefficient of diffusion in the mixture, C is the species concentration, σ is the electrical conductivity, B_o is the externally imposed magnetic field in the y -direction, k_T is the thermal-diffusion ratio, c_s is the concentration susceptibility, c_p is the specific heat at constant pressure and T_m is the mean fluid temperature. We introduce the following non-dimensional variables;

$$\eta = \sqrt{\frac{B}{\nu}} y, F(\eta) = \frac{\psi}{x\sqrt{B\nu}}, \theta(\eta) = \frac{T - T_\infty}{T_w - T_\infty}, \phi(\eta) = \frac{C - C_\infty}{C_w - C_\infty}, \quad (6)$$

where $F(\eta)$ is a dimensionless stream function, $\theta(\eta)$ is a dimensionless temperature of the fluid in the boundary layer region, $\phi(\eta)$ is a dimensionless species concentration of the fluid in the boundary layer region and η is the similarity variable. The velocity components u and v are respectively obtained as follows

$$u = \frac{\partial \psi}{\partial y} = xBF', v = -\frac{\partial \psi}{\partial x} = -\sqrt{B\nu}F, \quad (7)$$

where $F_w = \frac{V}{\sqrt{B\nu}}$ is the dimensionless suction velocity.

Following eq.(6), the partial differential equations (2)-(4) are transformed into local similarity equations as follows:

$$F''' + FF'' - (F' + M)F' + G_c\theta + G_c\phi = 0 \quad (8)$$

$$\theta'' + \text{Pr}(F\theta' - F'\theta) + \text{Pr}Du\phi'' = 0 \quad (9)$$

$$\phi'' + \text{Sc}(F\phi' - F'\phi) + \text{Sc}Sr\theta'' = 0, \quad (10)$$

where primes denote differentiation with respect to η . The appropriate flat, free convection boundary conditions are also transformed into the form,

$$\begin{aligned}
&F'=1, F=-F_w, \theta=1, \phi=1 \text{ at } \eta=0 \\
&F'=0, \theta=0, \phi=0 \text{ as } \eta \rightarrow \infty,
\end{aligned} \tag{11}$$

where $M = \frac{\sigma B_o^2}{\rho B}$ is the magnetic parameter,

$Pr = \frac{\nu}{\alpha}$ is the Prandtl number,

$Sc = \frac{\nu}{D_m}$ is the Schmidt number,

$G_r = \frac{g\beta_T(T_w - T_\infty)}{xB^2}$ is the local temperature Grashof number,

$G_c = \frac{g\beta_c(C_w - C_\infty)}{xB^2}$ is the local concentration Grashof number,

$D_u = \frac{D_m k_T (C_w - C_\infty)}{c_s c_p (T_w - T_\infty)}$ is the Dufour number,

$S_r = \frac{D_m k_T (T_w - T_\infty)}{T_m (C_w - C_\infty) \nu}$ is the Soret number.

The quantities of physical interest in this problem are local skin friction, the local Nusselt number, and the local Sherwood number.

3. Numerical methods for solution

Eqs. (8)-(10) constitute a highly non-linear coupled boundary value problem of third and second-order. So we develop most effective numerical shooting technique with sixth-order Runge-Kutta integration algorithm. To select η_∞ we begin with some initial guess value and solve the problem with some particular set of parameters to obtain $F''(0), \theta'(0)$ and $\phi'(0)$. The solution process is repeated with another larger value of η_∞ until two successive values of $F''(0), \theta'(0)$ and $\phi'(0)$ differ only after desired digit signifying the limit of the boundary along η . The last value of η_∞ is chosen as appropriate value for that particular simultaneous equations of first order for seven unknowns following the method of superposition [25]. To solve this system we require seven initial conditions whilst we have only two initial conditions $F'(0)$ and $F(0)$ on F , two initial conditions on each on θ and ϕ . Still there are three initial conditions $F''(0), \theta'(0)$ and $\phi'(0)$ which are not prescribed. Now, we employ numerical shooting technique where these two ending boundary conditions are utilized to produce two unknown initial conditions at $\eta = 0$. In this

1
2
3
4 calculation, the step size $\Delta\eta=0.001$ is used while obtaining the numerical solution with
5
6 $\eta_{\max}=11$ and five-decimal accuracy as the criterion for convergence.
7
8
9

10 **4. Results and discussion**

11
12 Numerical calculations have been carried out for different values of the thermophysical
13 parameters controlling the fluid dynamics in the flow regime. The values of Schmidt number
14 (Sc) are chosen for hydrogen ($Sc = 0.22$), water vapour ($Sc = 0.62$), ammonia ($Sc = 0.78$) and
15 Propyl Benzene ($Sc = 2.62$) at temperature 25°C and one atmospheric pressure. The values of
16 Prandtl number is chosen to be $Pr = 0.72$ which represents air at temperature 25°C and one
17 atmospheric pressure. Attention is focused on positive values of the buoyancy parameters i.e.
18 Grashof number $Gr > 0$ (which corresponds to the cooling problem) and solutal Grashof number
19 $G_c > 0$ (which indicates that the chemical species concentration in the free stream region is less
20 than the concentration at the boundary surface). The cooling problem is often encountered in
21 engineering applications; for example in the cooling of electronic components and nuclear
22 reactors. In all computations we desire the variation of F , θ and ϕ versus η for the velocity,
23 temperature and species diffusion boundary layers. Table (1) shows the comparison of Ibrahim
24 and Makinde [23] work with the present work for Prandtl number ($Pr= 0.72$) and it is noteworthy
25 that there is a perfect agreement in the absence of Dufour and Soret. From table (2), it is seen
26 that the local skin friction together with the heat and mass transfer rate at the moving plate
27 surface decreases with increasing magnitude of fluid suction (F_w) at the moving surface while
28 surface increasing with decreasing magnitude of fluid injection at the moving surface. The rate
29 of heat and mass transfer at the plate surface increases with increasing intensity of buoyancy
30 forces (Gr , G_c), decreases with increasing intensity of magnetic field (M), Dufour and Soret
31 numbers (Du , Sr). Moreover, the skin friction decreases with buoyancy forces and increases with
32
33 Increasing magnetic field intensity and Schmidt number (Sc). Finally, we observed that the flow
34 field is appreciably influenced by the Dufour and Soret effects. Therefore, we can conclude that
35 for fluids of hydrogen-air mixtures, the Dufour and Soret effects should not be neglected.
36 Furthermore, the surface mass transfer rate increases while the surface heat transfer rate
37 decreases with an increase in the Schmidt number. From Table (3), it was observed that the
38 suction parameter ($F_w > 0$) tends to increase the local skin friction, while the opposite trend is
39
40
41
42
43
44
45
46
47
48
49
50
51
52
53
54
55
56
57
58
59
60
61
62
63
64
65

observed for the injection parameter ($F_w < 0$). This is because blowing gives rise to a thicker velocity boundary layer, thereby causing a decrease in the velocity gradient at the surface. The local Nusselt number increases at the negative value of the suction parameter, while it decreases at the positive value of the injection parameter. This is because as the injection is applied at the surface, the momentum transport is reduced near the surface thereby causing a reduction in the local Nusselt number. Similarly, the local Sherwood number increases when suction parameter is present, while it decreases when the surface is subjected to injection parameter.

Table 1: Computation showing comparison with Ibrahim & Makinde [23] of $F''(0)$, $\theta'(0)$ and $\phi'(0)$ for various values of embedded parameter for $Pr=0.72$, $Sr=0$, and $Du=0$

					Present	Present	Present	I&M[23]	I&M[23]	I&M[23]
Gr	Gc	M	F_w	Sc	$-F''(0)$	$-\theta'(0)$	$-\phi'(0)$	$-F''(0)$	$-\theta'(0)$	$-\phi'(0)$
0.1	0.1	0.1	0.1	0.62	0.88908545	0.79653042	0.72547664	0.888971	0.7965511	0.7253292
0.5	0.1	0.1	0.1	0.62	0.69603619	0.83787782	0.76585079	0.695974	0.8379008	0.7658018
1.0	0.1	0.1	0.1	0.62	0.47509316	0.87526944	0.80202587	0.475058	0.8752835	0.8020042
0.1	0.5	0.1	0.1	0.62	0.68702142	0.84207706	0.77016532	0.686927	0.8421370	0.7701717
0.1	1.0	0.1	0.1	0.62	0.45778202	0.88182384	0.80871749	0.457723	0.8818619	0.8087332
0.1	0.1	1.0	0.1	0.62	1.26462533	0.70938977	0.64116350	1.264488	0.7089150	0.6400051
0.1	0.1	3.0	0.1	0.62	1.86838864	0.58541218	0.52519379	1.868158	0.5825119	0.5204793
0.1	0.1	0.1	1.0	0.62	0.57074524	0.56010990	0.52730854	0.570663	0.5601256	0.5271504
0.1	0.1	0.1	3.0	0.62	0.27515400	0.29557231	0.29025308	0.275153	0.2955702	0.2902427
0.1	0.1	0.1	0.1	0.78	0.89351757	0.79373969	0.83398390	0.893454	0.7936791	0.8339779
0.1	0.1	0.1	0.1	2.62	0.91236953	0.78489176	1.65041891	0.912307	0.7847840	1.6504511

Table 2: Computation showing $F''(0)$, $\theta'(0)$ and $\phi'(0)$ for various values of embedded parameter

Gr	Gc	M	F_w	Sc	Pr	Sr	Du	$-F''(0)$	$-\theta'(0)$	$-\phi'(0)$
0.1	0.1	0.1	0.1	0.62	0.72	0.1	0.03	0.88743829	0.78854903	0.69526904
0.5	0.1	0.1	0.1	0.62	0.72	0.1	0.03	0.69354257	0.82992680	0.73536678
1.0	0.1	0.1	0.1	0.62	0.72	0.1	0.03	0.47168842	0.86730429	0.77114416
0.1	0.5	0.1	0.1	0.62	0.72	0.1	0.03	0.68184199	0.83527987	0.74089827
0.1	1.0	0.1	0.1	0.62	0.72	0.1	0.03	0.44921329	0.87564043	0.77968381
0.1	0.1	1.0	0.1	0.62	0.72	0.1	0.03	1.26355437	0.70177349	0.61218037
0.1	0.1	3.0	0.1	0.62	0.72	0.1	0.03	1.86786443	0.57862504	0.49948379
0.1	0.1	0.1	1.0	0.62	0.72	0.1	0.03	0.57021615	0.55630816	0.51327770
0.1	0.1	0.1	3.0	0.62	0.72	0.1	0.03	0.27512619	0.29487694	0.28789907
0.1	0.1	0.1	-0.1	0.62	0.72	0.1	0.03	0.98394287	0.85469292	0.74626691
0.1	0.1	0.1	-1.0	0.62	0.72	0.1	0.03	1.54315969	1.22650204	1.03503982
0.1	0.1	0.1	0.1	0.78	0.72	0.1	0.03	0.89168750	0.78417217	0.79805392
0.1	0.1	0.1	0.1	2.62	0.72	0.1	0.03	0.90971550	0.76190308	1.56957263

0.1	0.1	0.1	0.1	0.62	1.0	0.1	0.03	0.89315322	0.95809716	0.68355351
0.1	0.1	0.1	0.1	0.62	3.0	0.1	0.03	0.90829074	1.75368367	0.63526228
0.1	0.1	0.1	0.1	0.62	7.0	0.1	0.03	0.91639143	2.67686061	0.58104858
0.1	0.1	0.1	0.1	0.62	0.72	0.4	0.03	0.88370546	0.79233598	0.60364269
0.1	0.1	0.1	0.1	0.62	0.72	2.0	0.03	0.86479566	0.81097022	0.10794354
0.1	0.1	0.1	0.1	0.62	0.72	0.1	0.15	0.88598564	0.75328336	0.69792631
0.1	0.1	0.1	0.1	0.62	0.72	0.1	0.60	0.88062396	0.61906425	0.70778467

Table 3: Results of $F''(0)$, $\theta'(0)$ and $\phi'(0)$ for various values of Fw ($Pr=0.72$, $Sc=0.62$, $Gr=0.1$, $Gc=0.1$, $M=0.1$, $Du=0.03$, $Sr=0.1$).

Fw	$-F''(0)$	$-\theta'(0)$	$-\phi'(0)$
0.5	0.724431308	0.67300439	0.60569621
0.3	0.801101962	0.72809519	0.64853672
0	0.934397731	0.82089177	0.72021233
-0.3	1.090853905	0.92677824	0.80186611
-0.5	1.208096735	1.00494205	0.86231477

A. Velocity Profiles

Figures 2-5 depict the effects of emerging flow parameters on non-dimensional velocity profiles. In figure 2 the effect of increasing the magnetic field strength and injection suction parameter on the momentum boundary-layer thickness is illustrated. Increasing the magnetic field strength parameter lead to a decrease in the velocity which confirmed with the fact that the magnetic field presents a damping effect on the velocity by creating a drag force that opposes the fluid motion. Figure 2 also shows an increase in the fluid velocity within the boundary layer due to suction and a decrease in the fluid velocity within the boundary layer due to injection. This indicates the usual fact that suction stabilizes the boundary layer growth. Furthermore, figure 3 shows that an increase in the buoyancy forces parameters lead to an increase in the velocity profile. It is established that increase in buoyancy forces enhancing the fluid flow. It was observed in Figure 4 that increases in Soret and Dufour numbers lead to an increase in the fluid flow causes the momentum boundary layer thickness generally increases away from the plate satisfying the boundary conditions. Figure 5 show the comparison between [23] and the present study when $Du = 0$, $Sr = 0$ and $Du = 0.6$, $Sr = 2$. It is clearly seen from the graph that when Soret and Dufour numbers were include the velocity boundary layer thickness increases across the plate.

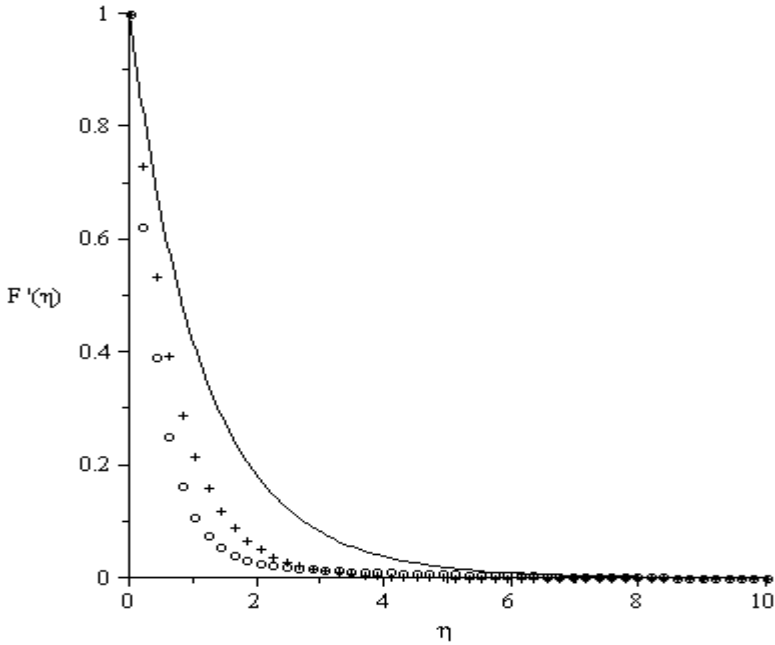


Figure 2: Velocity profiles of ——— $M=0.1, F_w=0.1$, ooooo $M=5, F_w=0.1$, +++++ $M=0.1, F_w=-1$ for fixed values of $Pr=0.72, Sc=0.62, Gr=Gc=0.1, Sr=0.1, Du=0.03$.

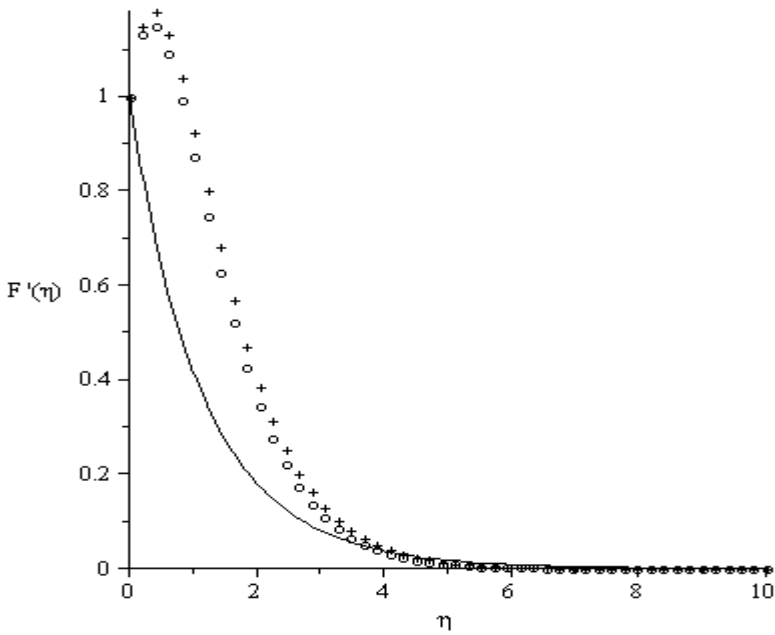


Figure 3: Velocity profiles of ——— $Gr=0.1, Gc=0.1$, ooooo $Gr=5, Gc=0.1$, +++++ $Gr=0.1, Gc=5$ for fixed values of $Pr=0.72, F_w=0.1, M=0.1, Sc=0.62, Du=0.03, Sr=0.1$.

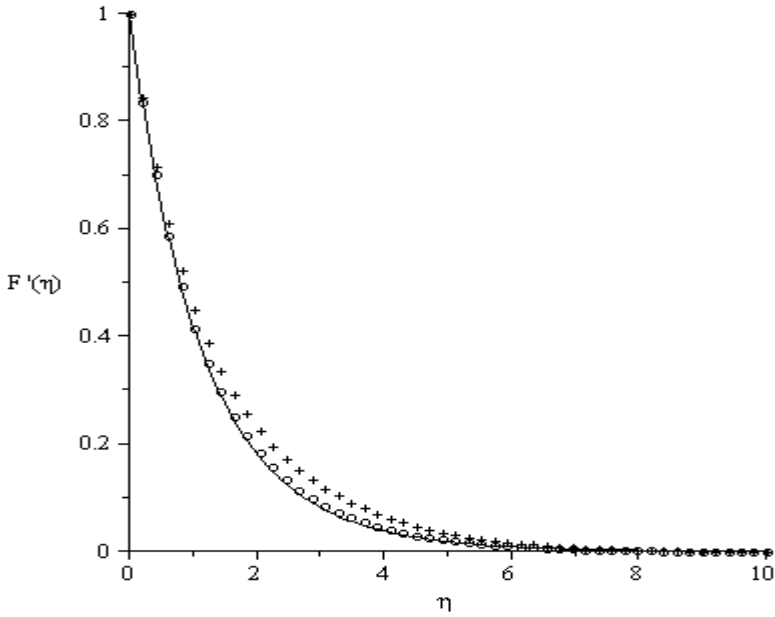


Figure 4: Velocity profiles of ——— $Du = 0.03, Sr = 0.1$, $\circ\circ\circ\circ Du = 0.6, Sr = 0.1$, $++++ Du = 0.03, Sr = 4$ for fixed values of $Pr = 0.72, Fw = 0.1, M = 0.1, Sc = 0.62, Gr = Gc = 0.1$.

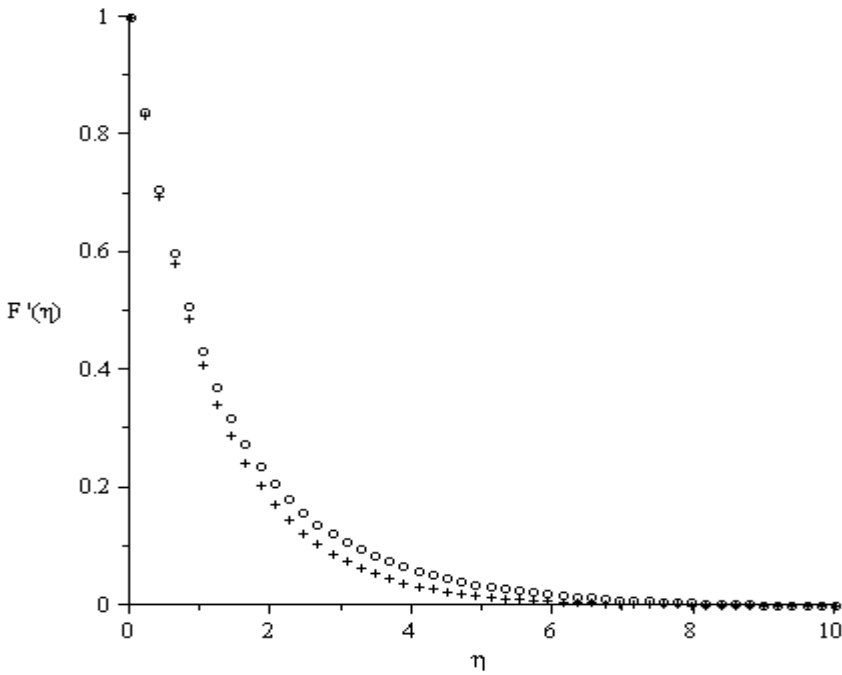


Figure 5: Velocity profiles of $++++ Pr = 0.72, Du = 0, Sr = 0$, $\circ\circ\circ\circ Pr = 0.72, Du = 0.6, Sr = 2$ for $M = Gr = Gc = Fw = 0.1, Sc = 0.62$.

B. Temperature Profiles

The effects of various thermophysical parameters on the fluid temperature are illustrated in Figures. 6 to 10. Generally, the fluid temperature increases from the plate surface and attained its peak value at the free stream whenever the plate surface temperature θ_w is lower than the free stream temperature. Figure 6 shows the influence of magnetic field strength and the suction parameter on the temperature profile. It is clearly seen that increasing the magnetic field strength increases the thermal boundary layer thickness across the plate while suction parameter decreases the temperature. In figures 7, we observed that an increase in both thermal and solutal Grashof number brings a decrease in the fluid temperature with an increase in the intensity of buoyancy forces. Figure 8 shows the influence of Dufour and Soret numbers on fluid temperature. We observed an increase in the fluid temperature with an increase in the Dufour number while a decrease in fluid temperature when the Soret number increases. The effect of Schmitz number and Prandtl number is illustrated in figure 9. We observed that increase in Prandtl number causes the thermal boundary layer thickness to increase thereby increases the fluid temperature and Schmitz number has little influence on the fluid temperature. Figure 10 show the comparison between [23] and the present study when $Du = 0$, $Sr = 0$ and $Du = 0.6$, $Sr = 2$. It is clearly seen from the graph that when Soret and Dufour numbers were include the thermal boundary layer thickness increases across the plate.

1
2
3
4
5
6
7
8
9
10
11
12
13
14
15
16
17
18
19
20
21
22
23
24
25
26
27
28
29
30
31
32
33
34
35
36
37
38
39
40
41
42
43
44
45
46
47
48
49
50
51
52
53
54
55
56
57
58
59
60
61
62
63
64
65

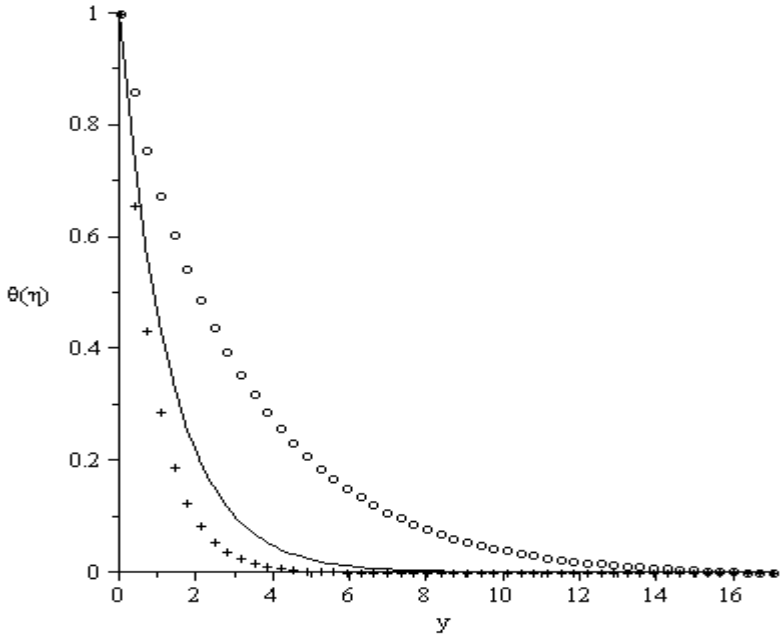


Figure 6: Temperature profiles of ——— $M=0.1$, $F_w=0.1$, ooooo $M=5$, $F_w=0.1$, ++++++ $M=0.1$, $F_w=-1$ for fixed values of $Pr=0.72$, $Sc=0.62$, $Gr=G_c=0.1$, $Sr=0.1$, $Du=0.03$.

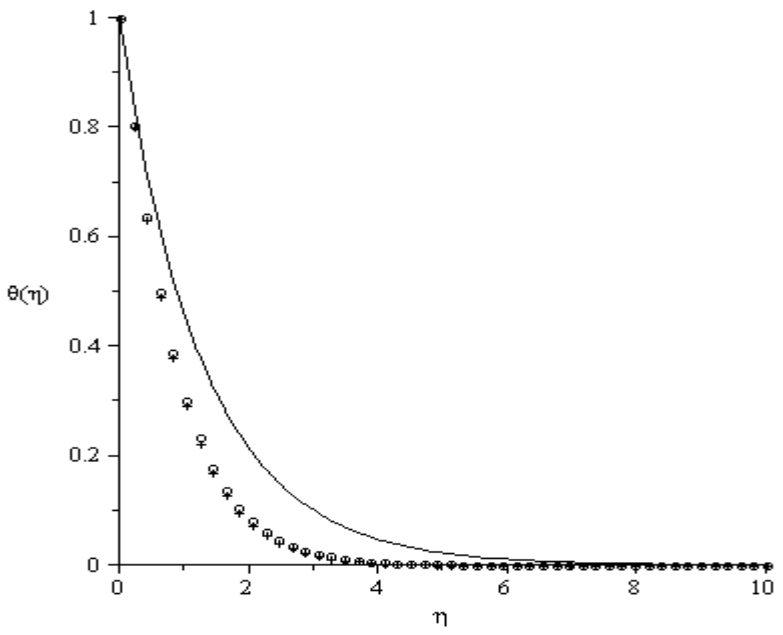


Figure 7: Temperature profiles of ——— $Gr=0.1$, $G_c=0.1$, ooooo $Gr=5$, $G_c=0.1$, +++++ $Gr=0.1$, $G_c=5$ for fixed values of $Pr=0.72$, $F_w=0.1$, $M=0.1$, $Sc=0.62$, $Du=0.03$, $Sr=0.1$.

1
2
3
4
5
6
7
8
9
10
11
12
13
14
15
16
17
18
19
20
21
22
23
24
25
26
27
28
29
30
31
32
33
34
35
36
37
38
39
40
41
42
43
44
45
46
47
48
49
50
51
52
53
54
55
56
57
58
59
60
61
62
63
64
65

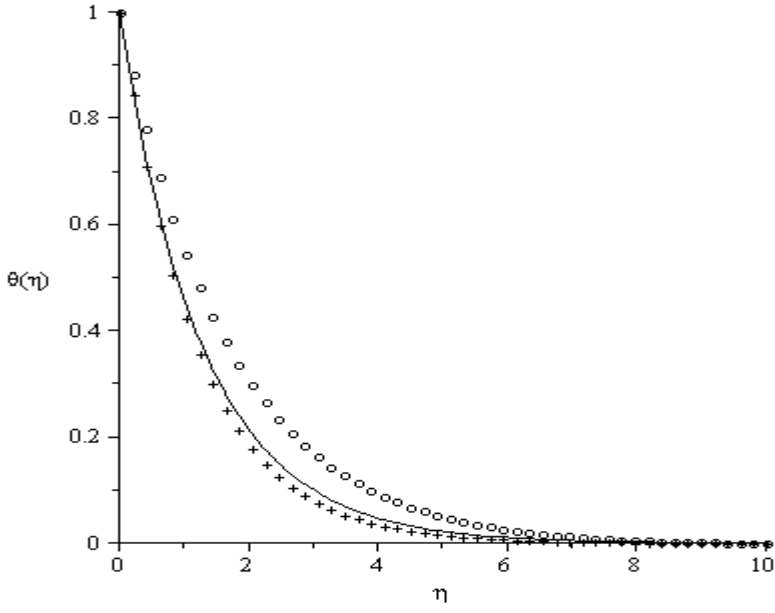


Figure 8: Temperature profiles of ——— $Du = 0.03, Sr = 0.1$, ooooo $Du = 0.6, Sr = 0.1$,
++++ $Du = 0.03, Sr = 4$ for fixed values of $Pr = 0.72, Fw = 0.1, M = 0.1, Sc = 0.62, Gr = Gc = 0.1$.

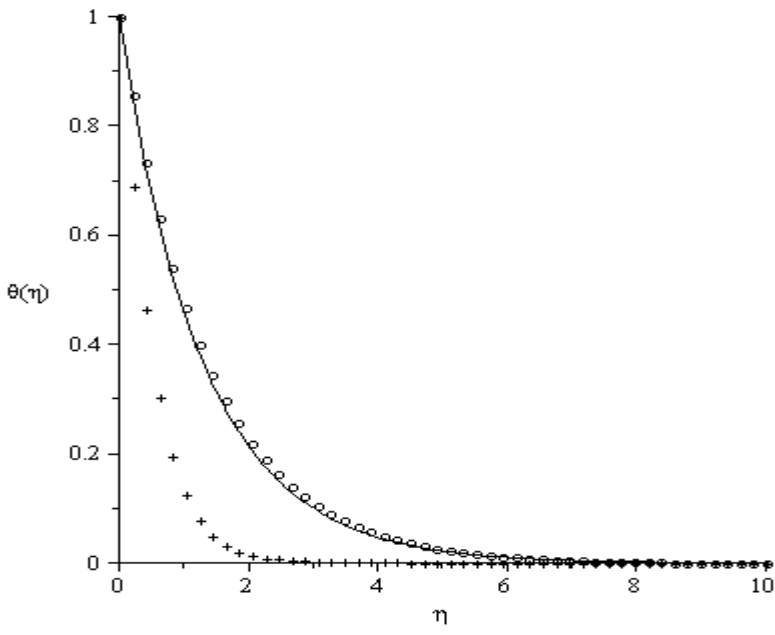


Figure 9: Temperature profiles of ——— $Sc = 0.62, Pr = 0.72$, ooooo $Sc = 2.62, Pr = 0.72$,
++++ $Sc = 0.62, Pr = 3$ for fixed values of $Fw = 0.1, M = 0.1, Gr = Gc = 0.1, Du = 0.03, Sr = 0.1$.

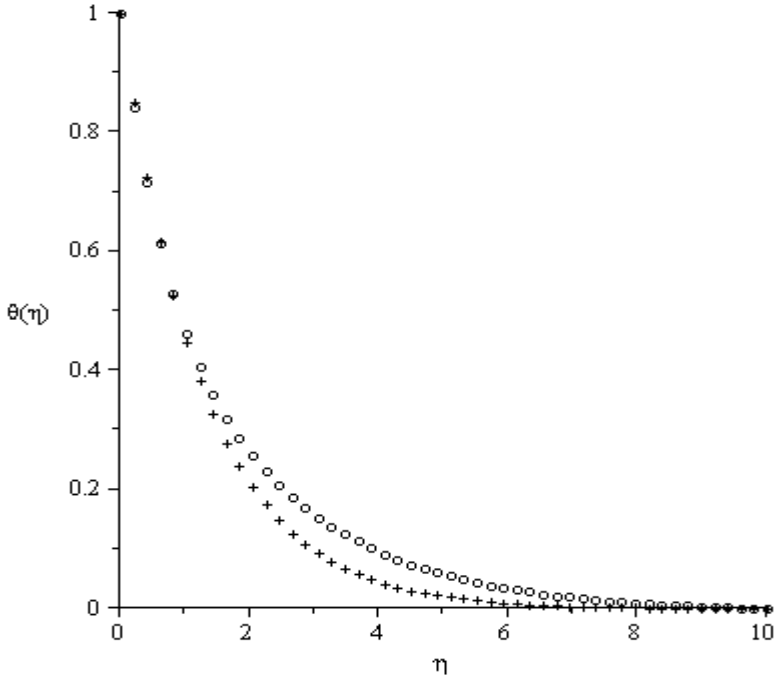


Figure 10: Temperature profiles of +++++Pr = 0.72, Du = 0, Sr = 0, oooooPr = 0.72, Du = 0.6, Sr = 2 for M = Gr = Gc = Fw = 0.1, Sc = 0.62.

C. Concentration Profiles

Figures 11–15 depict chemical species concentration profiles against spanwise coordinate η for varying values of physical parameters in the boundary layer. It is noteworthy that the species concentration increases from the plate surface and attained its peak value at free stream whenever the concentration at the plate surface ϕ_w is lower than that of the free stream. Figure 11 shows the influence of the magnetic field strength and suction parameter on the species concentration. Increase in magnetic field strength brings an increase in the species concentration boundary layer thickness while injection parameter decreases the chemical species concentration within the boundary layer and subsequent decaying of concentration boundary layer thickness. In figure 12, the concentration boundary layer thickness decreases with an increase in the thermal and solutal Grashof number across the plate. In figures 13, we observed an increase in concentration boundary layer thickness as Soret number increases while little or no effect was observed with increase in Dufour number. Figure 14 described the influence of Schmidt number and Prandtl number on the species concentration and it was observed that increase in Schmidt number leads to a decrease in the species concentration within the boundary layer due to the

combined effects of buoyancy forces and species molecular diffusivity. Figure 15 demonstrate the effects of Dufour and Soret numbers on the species concentration boundary layer thickness when $Pr = 0.72$, $Du = 0$, $Sr = 0$ and $Pr = 0.72$, $Du = 0.6$, $Sr = 2$. It was observed that the effects of these two parameters on concentration boundary layer thickness cannot be under estimated.

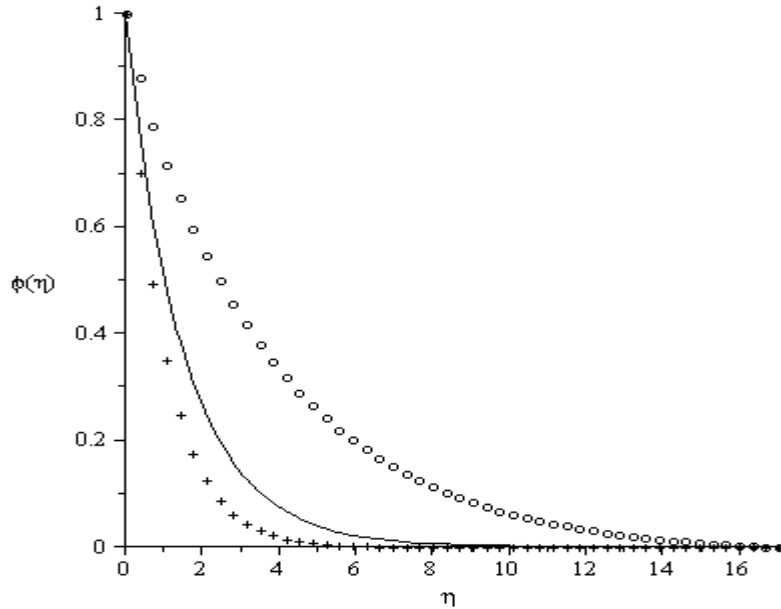


Figure 11: Concentration profiles of $\phi(\eta)$ vs η for $M=0.1, Fw=0.1$ (solid line), $M=5, Fw=0.1$ (dashed line), $M=0.1, Fw=-1$ (dotted line) for fixed values of $Pr=0.72, Sc=0.62, Gr=Gc=0.1, Sr=0.1, Du=0.03$.

1
2
3
4
5
6
7
8
9
10
11
12
13
14
15
16
17
18
19
20
21
22
23
24
25
26
27
28
29
30
31
32
33
34
35
36
37
38
39
40
41
42
43
44
45
46
47
48
49
50
51
52
53
54
55
56
57
58
59
60
61
62
63
64
65

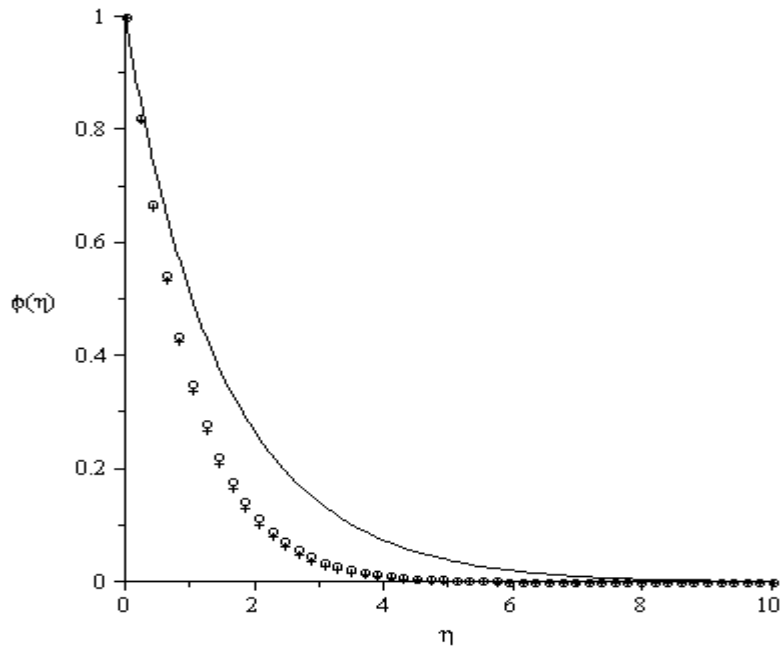


Figure 12: Concentration profiles of $\phi(\eta)$ vs η for $Gr = 0.1, Gc = 0.1$, $\circ\circ\circ\circ Gr = 5, Gc = 0.1$, $++++Gr = 0.1, Gc = 5$ for fixed values of $Pr = 0.72, Fw = 0.1, M = 0.1, Sc = 0.62, Du = 0.03, Sr = 0.1$.

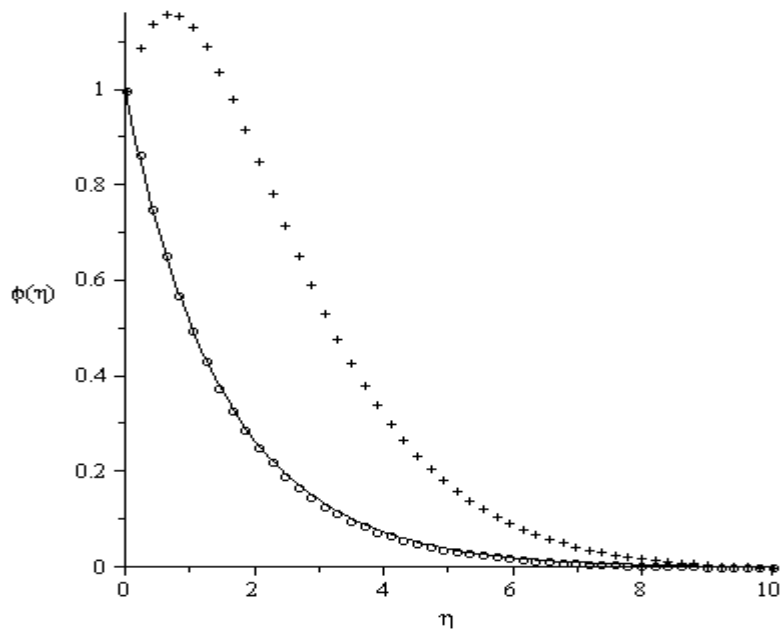


Figure 13: Concentration profiles of $\phi(\eta)$ vs η for $Du = 0.03, Sr = 0.1$, $\circ\circ\circ\circ Du = 0.6, Sr = 0.1$, $++++Du = 0.03, Sr = 4$ for fixed values of $Pr = 0.72, Fw = 0.1, M = 0.1, Sc = 0.62, Gr = Gc = 0.1$.

1
2
3
4
5
6
7
8
9
10
11
12
13
14
15
16
17
18
19
20
21
22
23
24
25
26
27
28
29
30
31
32
33
34
35
36
37
38
39
40
41
42
43
44
45
46
47
48
49
50
51
52
53
54
55
56
57
58
59
60
61
62
63
64
65

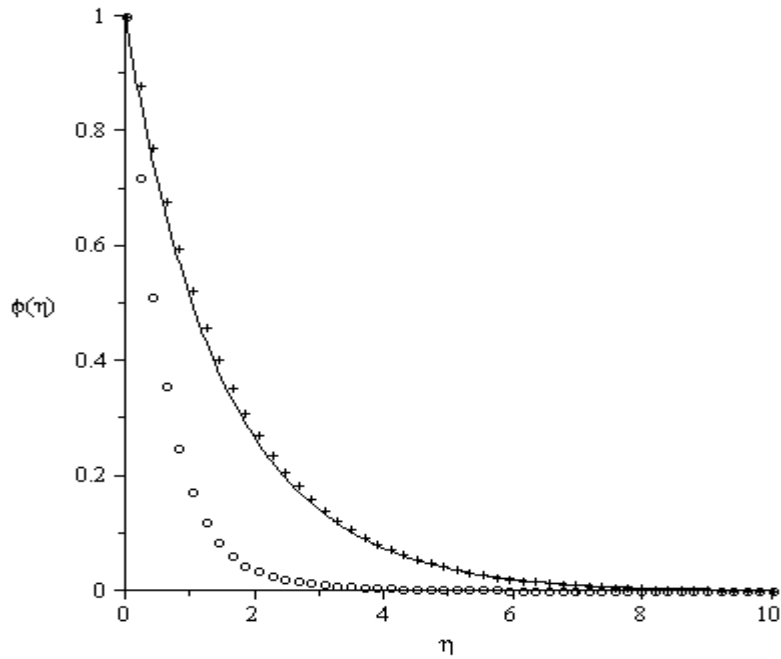


Figure 14: Concentration profiles of ——— $Sc = 0.62, Pr = 0.72$, ooooo $Sc = 2.62, Pr = 0.72$,
+++++ $Sc = 0.62, Pr = 3$ for fixed values of $F_w = 0.1, M = 0.1, Gr = G_c = 0.1, Du = 0.03, Sr = 0.1$.

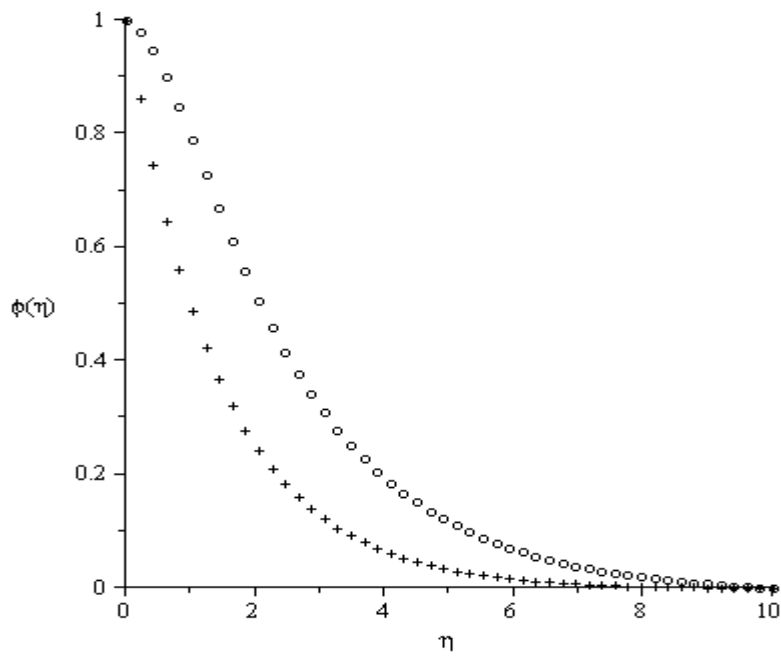


Figure 15: Concentration profiles of +++++ $Pr = 0.72, Du = 0, Sr = 0$, ooooo $Pr = 0.72, Du = 0.6,$
 $Sr = 2$ for $M = Gr = G_c = F_w = 0.1, Sc = 0.62$.

5 Conclusions

In this paper, we discussed MHD free convective heat and mass transfer past a moving vertical plate with Soret and Dufour effect in the presence of suction/injection parameter. The effects of thermal-diffusion and diffusion thermo with suction/injection parameter are investigated. Similarity solutions are obtained using scaling transformations. The set of governing equations and the boundary condition are reduced to ordinary differential equations with appropriate boundary conditions. Influence of Soret number, Dufour number, suction/injection parameter, Schmidt number, Prandtl number, magnetic parameter on MHD free convective heat and mass transfer have been discussed in detail. It was observed that the skin friction coefficient, the local Nusselt number decreases by increasing Dufour number and decreasing Soret number. We observed that in table 1, there are excellent agreement with Ibrahim and Makinde [23]. Finally, in the presence of a magnetic field, the fluid velocity is found to be decreased, associated with a reduction in the velocity gradient at the wall, and thus the local skin-friction coefficient decreases. Similarly, we experienced a decrease in the wall temperature gradient and concentration gradient due to applied magnetic field which yield a decrease in the local Nusselt number and the local Sherwood number.

Acknowledgement

OPO want to thank for the financial support of Covenant University, Ota. Nigeria.

References

- [1] Nield D.A., Bejan A. Convection in porous media. 3rd ed. New York: Springer; 2006.
- [2] Ingham D.B., Pop I., Transport phenomena in porous media, vol. III. Oxford: Pergamon; 2005.
- [3] Vafai K, Handbook of porous media. New York: Taylor & Francis; 2005.
- [4] Pop I., Ingham D.B., Convective heat transfer: mathematical and computational modeling of viscous fluids and porous media. Oxford: Pergamon; 2001.
- [5] Bejan A., Dincer I., Lorente S, Miguel A.F., Reis A.H. Porous and complex flow structures in modern technologies. New York: Springer; 2004.
- [6] Ingham D. B., Bejan A., Mamut E., Pop I., Emerging technologies and techniques in porous media. Dordrecht: Kluwer; 2004.
- [7] Vadasz P, Emerging topics in heat and mass transfer in porous media. New York: Springer; 2008.

- 1
2
3
4 [8] Chakrabarti A, Gupta AS. Hydromagnetic flow and heat transfer over a stretching sheet. Q
5 Appl Math, Vol. 37, 73–78, 1979.
6
7 [9] Sakiadis BC. Boundary layer behavior on continuous solid surfaces I. Boundary layer
8 equations for two-dimensional and axisymmetric flow. AICHE J. Vol. 7, 26–28, 1961.
9
10 [10] Chiam TC. Hydrodynamic flow over a surface stretching with a power law velocity. Int J
11 Eng Sci., Vol.33, 429–35, 1995.
12
13
14
15 [11] Makinde O.D., MHD steady flow and heat transfer on the sliding plate. A.M.S.E.,
16 Modelling, Measurement & Control B. Vol. 70, No. 1, 61-70, 2001.
17
18
19
20 [12] Makinde O.D., Magneto-Hydrodynamic Stability of plane-Poiseuille flow using Multi-Deck
21 asymptotic technique. Mathematical & Computer Modelling Vol. 37, No. 3-4, 251-259, 2003.
22
23
24 [13] Makinde O.D., Effect of arbitrary magnetic Reynolds number on MHD flows in convergent-
25 divergent channels. International Journal of Numerical Methods for Heat & Fluid Flow, Vol. 18,
26 No. 6, 697-707, 2008.
27
28
29
30 [14] Makinde O.D., On MHD boundary-layer flow and mass transfer past a vertical plate in a
31 porous medium with constant heat flux. Int. J. Num. Methods for Heat & Fluid Flow, Vol. 19,
32 Nos 3/4, 546-554, 2009.
33
34
35 [15] Sparrow E.M., Cess R.D., The effect of a magnetic field on free convection heat transfer.
36 Int. J. Heat Mass Transfer, Vol.4, 267-274, 1961.
37
38
39 [16] Yih K.A., Free convection effect on MHD coupled heat and mass transfer of a moving
40 permeable vertical surface. Int. Commun Heat Mass Transfer, Vol. 26(1), 95-104, 1999.
41
42
43 [17] Alam M.S., Rahman M.M., Dufour and Soret effects on mixed convection flow past a
44 vertical porous flat plate with variable suction. Nonlinear Analysis: Modelling and Control, Vol.
45 11, No. 1, 3-12, 2006.
46
47
48 [18] Gaikwad S.N., Malashetty M.S., Prasad K. R, An analytical study of linear and non-linear
49 double diffusive convection with Soret and Dufour effects in couple stress fluid. International
50 Journal of Non-Linear Mechanics, Vol. 42, 903-913, 2007.
51
52
53
54
55
56
57
58
59
60
61
62
63
64
65

1
2
3
4 [19] Osalusi E., Side J, Harris R., Thermal-diffusion and diffusion-thermo effects on combined
5 heat and mass transfer of a steady MHD convective and slip flow due to a rotating disk with
6 viscous dissipation and Ohmic heating. International Communications in Heat and Mass
7 Transfer, Vol. 35, 908-915, 2008.
8
9

10
11
12 [20] Beg A. O., Bakier A.Y., Prasad V.R., Numerical study of free convection
13 magnetohydrodynamic heat and mass transfer from a stretching surface to a saturated porous
14 medium with Soret and Dufour effects. Computational Material Science, Vol. 46, 57-65, 2009.
15
16
17

18
19 [21] Nithyadevi N., Yang Ruey-Jen. Double diffusive natural convection in a partially heated
20 enclosure with Soret and Dufour effects. International Journal of Heat and Fluid Flow, 2009 (In
21 Press).
22
23

24
25 [22] Olanrewaju P. O., Dufour and Soret Effects of a Transient Free Convective Flow with
26 Radiative Heat Transfer Past a Flat Plate Moving Through a Binary Mixture. Pacific Journal of
27 Science and Technology, Vol. 11. No. 1, 2010.
28
29

30 [23] Ibrahim S. Y., Makinde O. D., Chemically reacting MHD boundary layer flow of heat and
31 mass transfer past a moving vertical plate with suction. Scientific Research and Essay, Vol. 5(19)
32 2875-2882 2010.
33
34
35

36
37 [24] Kafoussias NG, Williams EW. Thermal-diffusion and diffusion-thermo effects on mixed
38 free-convective and mass transfer boundary layer flow with temperature dependent viscosity. Int.
39 J Eng Sci 1995; 33: 1369-84.
40
41

42
43 [25] Na TY. Computational methods in engineering boundary value problems. New York:
44 Academic Press; 1979.
45
46
47
48
49
50
51
52
53
54
55
56
57
58
59
60
61
62
63
64
65

Reviewer #1.

1. The figures have been redrawn as requested by the reviewer to reduce the number of figures and for easy understanding.

Reviewer #2.

1. See table 1 and figures 5, 10 and 15 for the comparison. It is clearly seen from eqs 3 and 4 that only one additional term was added to both equations that is different from [23] which represents the Dufour and Soret number in the dimensionless form which was neglected from their paper.
2. No except that Runge-Kutta of order sixth was used for better accuracy in this article while they used Runge-Kutta of order fourth [23].
3. In their study, Dufour and Soret effects were neglected, since they are of a smaller order magnitude than the effects described by Fourier's and Fick's law. There are, however, exceptions. The Soret effect, for instance, has been utilized for isotope separation and in a mixture between gases and with very light molecular weight (H₂, He) and of medium molecular weight (H₂, air) the Dufour effect was found to be of considerable magnitude such that cannot be neglected (see [17], [19] and [22]).
4. See figures 5, 10 and 15 for quick comparison.
5. Dufour and Soret effects were neglected i.e. $Du = 0$, $Sr = 0$ since they are of a smaller order magnitude than the effects described by Fourier's and Fick's law.